Statistical Analysis of the Whole Body Absorption Depending on Anatomical Human Characteristics at the Frequency of 2.1 GHz

A. El Habachi [1], E Conil[1], A. Hadjem[1], E Vazquez[2], M. F. Wong[1], A. Gati[1], G Fleury [2] and J. Wiart [1]

[1]WHIST Joint Laboratory between INSTITUT TELECOM and Orange Labs, France
[2] SUPELEC Gif-sur-Yvette, France

Corresponding author: joe.wiart@orange-ftgroup.com.

Abstract.
In this paper we propose an identification of morphological factors that may impact the Whole Body Specific Absorption Rate (WBSAR). The study is conducted for the case of an exposure to a front plane wave at the 2100MHz frequency carrier. This study is based on the development of different regression models for estimating the WBSAR as a function of morphological factors morphology. For this manner, a database of twelve anatomical human models (phantoms) has been considered. Also, eighteen supplementary phantoms obtained using morphing technique were generated to build the requested relation. The paper presents three models based on external morphological factors like the Body Surface Area (BSA), the Body Mass Index (BMI) or the body mass. These models show good results for families obtained by morphing technique on the estimation of the WBSAR (< 10%) but still less accurate (30%) when applied for different original phantoms. This study stresses the importance of the internal morphological factors such as muscle and fat proportions in the characterization of the WBSAR. The regression models are then improved using internal morphological factors with an estimation error around 10% on the WBSAR.
Finally, this study is suited for establishing the statistical distribution of the WBSAR for a given population characterized by its morphology.

Key words: Radiofrequencies, Specific Absorption Rate, Exposure, FDTD, Statistical analysis, Regression models.

1. Introduction

The technologies involving Electromagnetic Fields (EMF) propagation are increasingly used around the world. However, this huge growth induces a public concern about possible health effects.
To protect people from EMF overexposure, the International Commission on Non-Ionizing Radiation Protection (ICNIRP) and the Institute of Electrical and Electronic Engineers (IEEE) have defined limits. In the radiofrequencies domain, exposure to EMF is quantified by the Specific Absorption Rate (SAR) expressed in Watts per Kilogram. The Basic Restrictions (BR) are the fundamental limits expressed in term of the whole body averaged SAR as well as local SAR averaged on 1 or 10 grams of tissues.
BR are difficult to check in situ, hence the ICNIRP has also defined Reference Levels (RL) derived from BR [ICNIRP 1998]. RL give the maximum permissible electromagnetic field strength or power density (in the absence of a person). Compliance to RL is deemed to ensure compliance to BR. The link between reference levels and basic restrictions has been

established several years ago based on simplified human models and maximum coupling assumptions [Gandhi 1980].
Nowadays, computing resources have strongly increased, and large and complex problems (as the computation of the SAR induced in a 3D heterogeneous human body) can be analyzed in few hours. Numerical dosimetry is intensively used to analyze Specific Absorption Rate (SAR) distribution in tissues and to design exposure set up. Numerical methods, such as the well known Finite Difference in Time Domain (FDTD), enable to achieve a very good accuracy in the SAR computation. Based on that, several studies have used 3D human body models to analyze the relationship between the whole body averaged SAR (WBSAR) induced in a human model and the incident field. Recent studies have shown that the WBSAR induced by a plane wave with vertical electric field strength set to the reference levels can be non-conservative regarding the BR for some phantoms [Conil 2008, Dimbylow 2007]. These studies emphasize the variability of the WBSAR with frequency due to the variability of the morphology [Conil et al 2008].
Despite the development of computer resources, the number of human body models (a.k.a. phantoms) is still limited and the models have not been chosen using experimental design methods. Previous studies [Livingston and Lee 2001, Hirata et al 2007 and Hirata et al 2008] give some surrogate models to predict the WBSAR but usually; they are based on only a few phantoms or simplified geometry (such as spheroids).
In this paper we identify the morphological factors influencing the WBSAR for phantoms in a standing position and exposed to a plane wave, polarized vertically and arriving frontally. The frequency is fixed at 2100MHz with isolated conditions. This incidence is chosen since it is conservative compared to other direction of arrival [Conil et al 2009].
The objective is to build a model describing the WBSAR as a function of the morphology. The obtained result will allow to analyse and to extrapolate the exposure to large and different populations.
The method is based on the construction of regression models that makes it possible to estimate the statistical distribution of the WBSAR for a given human population.

2. Material

2.1. Phantoms

Only a few 3D heterogeneous human models exist worldwide, Most of these phantoms are based on MRI (Magnetic Resonance Imaging) but few such as the well known Visible Human [Ackerman 1995] are based on other methods. The figure 1 shows the twelve anatomical voxel models (3 females, 7 males and 2 children) used in this study. From left to right, the figure 1 shows the UK "Norman" model [Dimbylow 1997], the ETRI Korean male [Lee A.K 2006], the Japanese male "Taro" (JM) and female "Hanako" (JF) [Nagaoka et al 2004], the American Zubal model [Zubal et al 1994], the Visible Human (VH) from VH project [Ackerman 1995], the High Definition Reference Korean model (HDRK) [Kim et al 2008], the UK "Naomi" model [Dimbylow 2005a] and the Virtual Family models [Christ et al 2007] composed of two adults, a male "Duke", a female "Ella" and two children: a 11 years old girl "Billie" and a 6 years old boy "Thelonious" .

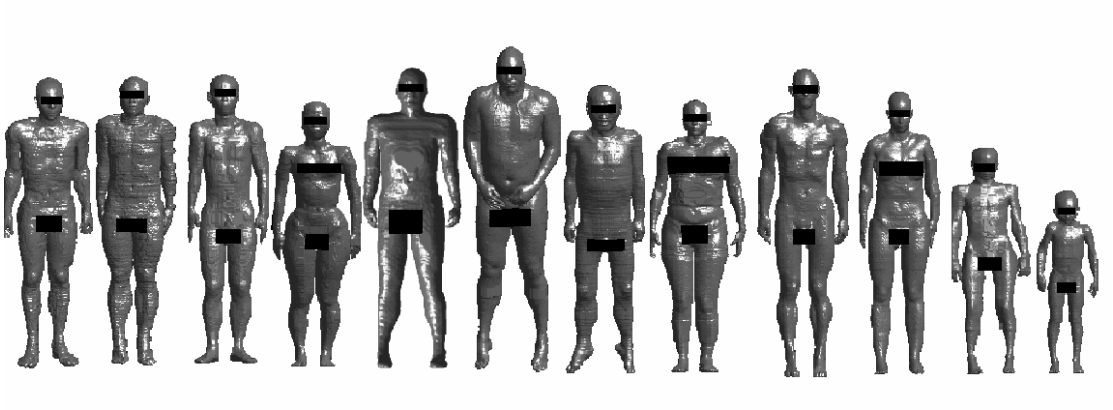

Figure 1. Illustration of the phantoms used in the study

In order to describe the WBSAR with a surrogate model taking into account the morphological data, the first step consists in characterizing these data and their influence. Two types of factors are distinguished: the internal (such as the masses of skin, muscles, fat and bones) and the external (such as height and total weight) ones. The influence of these factors may be significant.

Table 1 shows the proportion of the main internal (proportion of skin, muscles, fat and bones represent about 80% of the whole body weight) and external morphological factors of the phantoms used in this study. As shown in table 1, these factors vary considerably from one phantom to another (e.g. for the adult, the proportion of fat varies between 14% and 38% and the weight varies between 52 kg and 106 kg).

Table 1. Proportions of the main internal and external morphological factors of the phantoms used.

Phantoms	Height (cm)	Weight (kg)	Skin (%)	Fat (%)	Muscles (%)	Bones (%)
Norman	174	66	7.2	22	45	11.1
Zubal	175	81	5.7	21	42	17.4
Korean	176	76	11.8	14	47	15
VH	182	106	8.3	18	47	16
JM	173	67	5.5	29	43	10.3
JF	161	52	5.8	32	33	16.3
Ella	167	58	6.1	24	40	10.4
Duck	175	71	7.7	16.	48	12.4
Th	117	19	7.9	15	42	15.4
Billie	147	35	9.7	19	34	13.7
Naomi	158	64	5.1	38	32	14.7
HDRK	170	72	5.8	34	33	17.1

The International Commission on Radio Protection (ICRP) has published some mean values of masses of the main tissues for a population of North-Americans and European males [ICRP 2003]. The Table 2 compares the mean values of main tissue masses for the ICRP population with those computed for the 10 human adult models and their median used for this study.

As it can be seen, muscles and bones of the phantoms used in this study are close to the ICRP male population. For skin, difference exit and can be explain by the segmentation and voxel size. In this study the voxel size of the phantoms is equal to 2 millimetres that are much higher than the 1.2 millimetres of the skin thickness measured in the ICRP male population. Concerning the fat, the difference comes from the three females who are not included in the population of the ICRP male, and present a high mass of fat.

The comparison of the median of the phantom tissues with the mean of the ICRP male tissues shows that the distribution of the phantoms is quite symmetric around the mean of the ICRP population considering muscles, fat and bones. However, as explained before, the difference on skin still observed is due to the segmentation limitation.

Table 2. Mean factors extracted from ICRP and mean of adult phantoms factors.

	Ref. ICRP Male Mean	Phantoms mean	Phantoms median
Skin (kg)	3.3	4.8 (-31%)	4.46 (-26%)
Muscle(kg)	29.0	29 (0%)	28.7 (+1%)
Fat (kg)	14.6	18 (-19%)	14.41 (+1%)
Bones (kg)	10.5	9.9 (+6%)	10.19 (+1%)

Concerning the external morphological factors, factors such as weight, height, Body Mass Index (BMI) and Body Surface Area (BSA) are considered. The BMI and the BSA characterise respectively the fat proportion and the surface of the body. Different formulas are experimentally established in the literature to estimate the BSA. In our case, the formula of Dubois and Dubois [Dubois and Dubois 1916, Livingston and Lee 2001] is used. BMI and BSA are defined as a function of the height and the weight as given in equations 1 and 2.

$$BMI = \frac{weight(kg)}{height(m)^2}, \quad \textbf{(1)}$$

$$BSA(m^2) = 0.007184(weight_{kg}{}^{0.425} height_{cm}{}^{0.725}), \quad \textbf{(2)}$$

More information on these external morphological factors such as mean, standard deviation and sometimes percentiles are given for different populations in [Pineau and Kapitaniak 2004, Lim To et al 2000, Perissinoto et al 2001]. These statistical data are classified by origin, age or sex.

The analysis of these statistical data shows that BMI and weight can be described by normal distribution. Figures 2 and 3 show the Quantile to Quantile graphs (usually known as QQplot) of quantiles available on the BMI and the weight of a sample of Indian and Italian populations (the sizes of these samples are respectively 113 and 1666) compared to quantiles of theoretical normal distributions .Quantiles of the Indians BMIs are compared to those of normal distribution with mean of 20.91 and standard deviation of 3.4 and quantiles of the Italians weight are compared to those of the Normal distribution with mean of 66.7 and standard deviation of 10.7. The QQplot [Saporta 1990] is a technique that allows to check the correctness of a normal distribution assumption.

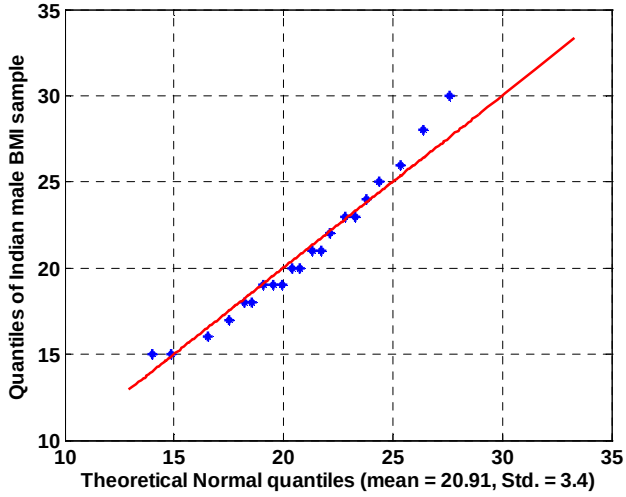

Figure 2. QQplot of Indian male BMI of age 20-24.

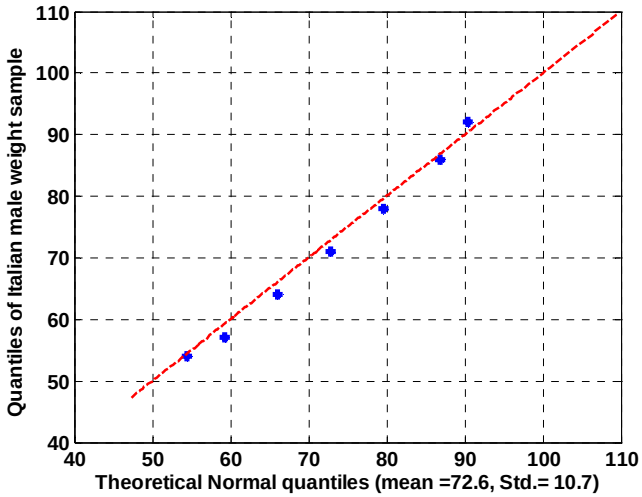

Figure 3. QQplot of Italian male weight of age 65-84.

The statistical distribution of all the morphological data is of great interest, since the quality of a surrogate model based on a set of phantoms depends on the representativeness of these phantoms. Moreover, such statistical distributions are also fundamental to determine the statistical distribution of the WBSAR. The figure 4 illustrates the dispersion of the BMI of the phantoms compared to the French population aged of 20 years (22.29±2.9), Italian 65-84 years (26.4±3.7) and Indian 20-24 years (20.91±3.4) [Pineau and Kapitaniak 2004, Lim To et al 2000, Perissinoto et al 2001].

As shown previously the BMI of Indian population 20-24 can be described by a Gaussian distribution. Hence, the BMI of these Italian, French and Italian populations is also assumed normal.

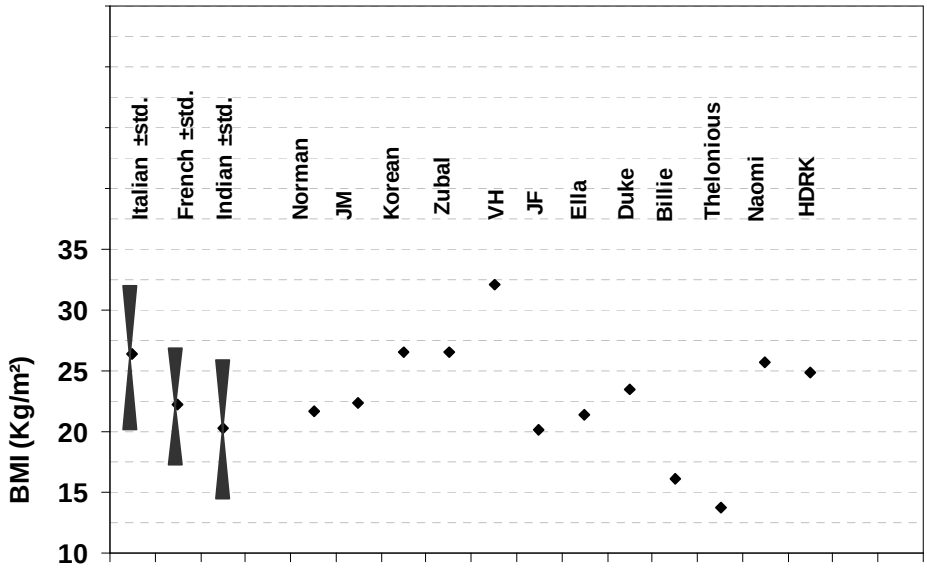

Figure 4. Dispersion of phantom BMI's in the French, Italian and Indian populations (± Std.).

The twelve phantoms have various origins (Asia, USA and Europe). Unfortunately, there is no statistical data on the BMI of the worldwide population. No test of the phantoms on the worldwide population can be performed and to test the phantoms on specific populations as French, Italian or Indian populations does not make sense. On the other hand, what is known is that most of the phantoms have been built to match the average man or woman of a given population (Norman is the Normalized Man, Japanese man and woman have been matched to the mean man and woman of the Japanese).

2.2. Morphed phantom

Since children phantoms are rare and difficult to obtain, morphing techniques [Hadjem et al 2004, Hirata et al 2007, Conil et al 2008, Wiart et al 2008, Wang et al 2006b] have been developed and used in several studies. This technique allows distorting external morphology by piecewise homothetic deformation of the body. In these studies, the morphing has been applied to obtain additional children at different ages.

Since the cross correlation of the external factors (such as height, shoulder width and shoulder dept and abdomen width and dept) in terms of age is not known, these additional phantoms are built using the external factors corresponding to the mean values of their class of age. Six families of phantoms have been created. Each family of phantoms is composed of an original adult phantom and the three morphed phantoms (aged of 5, 8 and 12 years of age). These families are based on the Japanese male, the Japanese female, Zubal, Visible Human, the Korean and Norman.

Figure 5 shows the Korean family (from left to right, we see the Korean children aged of 5, 8, 12 and on the right the adult Korean).

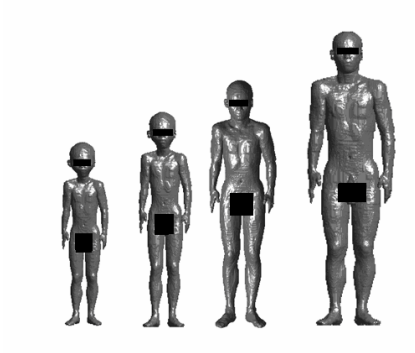

Figure 5. Example of the Korean family.

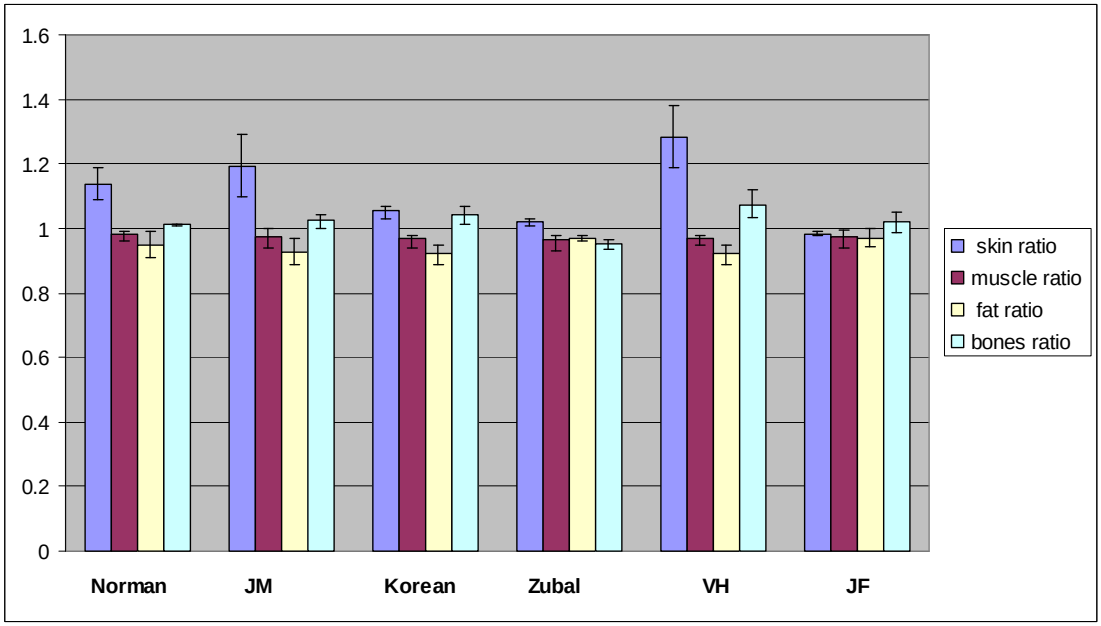

Figure 6. Ratio between the proportions tissue of morphed phantoms in each family and proportions tissue of the initial phantom in the same family (the error bar represents the maximal and minimal values of proportions ratio for each family).

Figure 6 shows that the tissues proportions of the morphed children derived from the same adult do not differ much (less than 8% except for the skin). Indeed, the ratio between the proportions of muscles, fat and bones for morphed children and the initial adult phantom close to 1. However, the ratio of the proportions of skin is larger for some families of phantom (Norman, JM and the VH family). These larger values of proportion skin ratio can be explained by the fact that the proportion of skin obtained on phantoms is small (between 5 and 7%, see table 1).

The proportions of internal tissues of the children phantoms obtained by the morphing technique are compared to those of the children of the virtual family that are based on MRI (the 5 years old children are compared to Thelonious aged of 6 and the 12 years old children are compared to Billie aged of 11).

To achieve this comparison, the test of Student is used. It tests the hypothesis that the sample comes from a distribution with fixed mean. Moreover this test is suitable in the case of a sample of small size (less than 30). The proportion of each tissue of Billie and Thelonious are considered as a mean target value of their class of age. The test of Student checks the hypothesis that the sample of the internal tissues of the morphed phantoms follows a normal distribution centered on the value given by the Virtual Family's children. Table 3 shows p-values of this test. A p-value larger than 0.05 allows accepting the hypothesis.

Table 3. P-value of the test of Student comparing the internal tissues of the virtual family children and those of the morphed phantoms.

	Comparison of the morphed phantoms aged of 5 years with Thelonious	Comparison of the morphed phantoms aged of 12 years with Billie
Skin	0.25	0.98
Muscle	0.52	0.78
Fat	0.64	0.06
Bones	0.39	0.39

The obtained p-value issue from the comparison of phantoms aged of 12 years with Billie is just accepted. This weak p-value can be explained by the fact that most of the morphed phantoms children are boys (5 boys and 1 girl). Furthermore, the fat proportions of females are generally higher than the fat proportions of males. This test of Student makes possible to validate that morphed phantoms are a sample of normal distribution with mean equal to the value of the phantoms children of the Virtual Family.

2.3. Whole Body SAR

To determine the power absorbed by the tissues of phantoms, the well known Finite Difference the Time Domain (FDTD) method has been used. FDTD has demonstrated its advantages in many EMF problems [Taflove 2000]. The FDTD is a numerical method allowing the resolution of Maxwell's equations in time domain. The fields *E* and *H* are discretized in space and time using the well known Yee scheme [Yee 1966]. Since the computational domain is limited, absorbing conditions have to be used to avoid spurious reflections at the boundary of the computational domain. In our case the well known PML (Perfectly-Matched Layer) have been used [Beranger 1994].
Locally the SAR is computed using the following formulation:

$$SAR = \frac{\sigma E^2}{2\rho}, \quad \textbf{(3)}$$

In this formulation σ, ρ and E represent respectively, the conductivity, the mass density of the tissue and the peak electric field strength.
The whole body averaged SAR is equal to the whole power absorbed by the phantom divided by his body weight.
As explained in the introduction, the phantoms are standing and they are exposed to a plane wave polarized vertically and arriving in front of them at the frequency of 2100 MHz. However, in [Conil et al 2009], the influence of the angle of incidence on the WBSAR has been studied and in [Kühn et al 2009] different polarizations have been analyzed.

3. Statistical analysis of the morphology influence on the WBSAR

3.1. Analysis of the external morphology

Recent publications show relationships between the WBSAR and the external morphology. These relations are based on the correlation between the absorbed power and the surface of the body.
In [Hirata et al 2007 and Hirata et al 2008], the surrogate model of the WBSAR is written as a linear function of the ratio BSA/weight. In this approach, the BSA is used as an estimator of the body surface. However, no statistical data for this ratio is available in the literature.
Other external factors like the BMI^{-1} are also used to estimate the WBSAR. This factor was first used to estimate the WBSAR in the 100MHz frequency range where some body resonance exist [Hirata et al 2008].
Furthermore, $weight^{-1/3}$ is as well used to estimate the WBSAR [Livingston et al 2001]. This factor comes from the proportionality relation between the body surface and $weight^{2/3}$ based

on the geometric relationship between the three-dimensional volume (proportional to body weight) and the two-dimensional body surface (i.e. proportional to body weight).
Finally, the given approaches are used to build the three following surrogate models.

$$y = \begin{cases} \alpha X_1 + \varepsilon, & (4) \\ \beta X_2 + \varepsilon' & \\ \gamma X_3, + \varepsilon'' & (5) \end{cases}$$

(6)

where :

- y, stands for the WBSAR
- α, β and γ are the unknown parameters of the models
- X_1, X_2 and X_3 are respectively, BSA/weight, BMI^{-1} and $weight^{-1/3}$
- ε, ε' and ε'' are the errors generated by the surrogate model (4), (5) and (6) respectively.

To estimate the parameters α, β and γ, the well known least square method is used. The estimation of these parameters generates an important error on the estimation of phantoms WBSAR (about 30%). Hence these factors are not enough to build an accurate surrogate model for the WBSAR.
However, the estimation of the parameters α, β and γ using one family of phantoms (cf. section 2.2) gives a very good estimation of the WBSAR (about 10% of error) for each family tested at 2100 MHz. Figure 7 shows the different regressions obtained for the families of phantoms using the external factors BSA/weight. Concerning the other factors we obtain similar results.

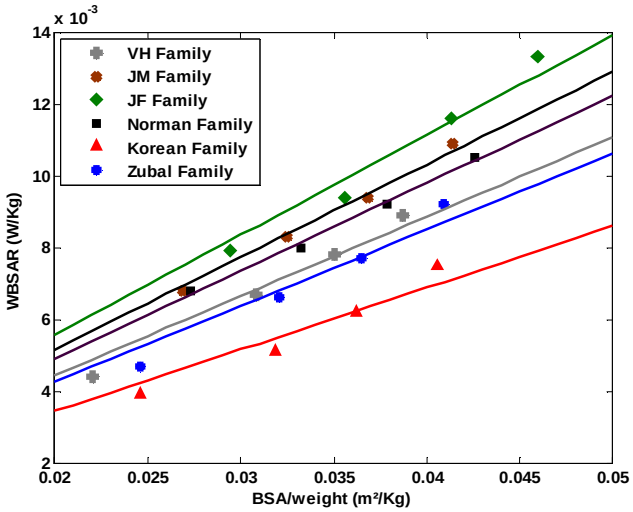

Figure 7. Relationship between BSA/weight and WBSAR (families of phantoms).

Table 4 gives the values of α, β and γ estimated by least square method and their corresponding R^2 for the families of phantoms.

Table 4. Estimation of the parameters α, β and γ, and the determination coefficient using family's phantoms on parameter.

	α (R^2)	β (R^2)	γ (R^2)
Norman family	0.24 (0.99)	0.15 (0.95)	0.0027 (0.99)
Korean family	0.17 (0.92)	0.11 (0.84)	0.0019 (0.93)
Zubal family	0.21 (0.94)	0.13 (0.90)	0.0023 (0.94)
VH family	0.22 (0.97)	0.15 (0.92)	0.0024 (0.96)
JM family	0.25 (0.99)	0.16 (0.91)	0.0029 (0.99)
JF family	0.28 (0.96)	0.16 (0.88)	0.0031 (0.96)

As discussed in section 2.2, for the families of phantoms, the internal tissues in terms of proportion, do not vary considerably because of the morphing technique. Hence in the models (4), (5) and (6), the terms α, β and γ depend strongly on the internal morphology.
Since the parameters α, β and γ are variable in terms of family, in the next section we will built a surrogate models for these parameters in term of internal morphology.

3.2. Analysis of internal morphology

The regressions established in the previous section, show a large variability of the parameters α, β and γ from one family to another. However, it is possible to use a fixed value of the parameters within each family of phantoms. The family dependence is due to the fact that the main tissues (fat, muscles and bones) weight proportions, as shown in section 2.2 are almost constant.
For this purpose, we build a model for the parameters α, β and γ in (4), (5) and (6), using the internal morphology. Equations (7), (8) and (9) describe the linear regression using the proportions of fat, muscle and bones (the main tissues of the human body) and the skin (the first exposed tissue):

$$\hat{\alpha} = \xi_1 + \xi_2(2x_S + x_M + x_F + \frac{3}{5}x_B) + \nu, \quad \textbf{(7)}$$

$$\hat{\beta} = \xi_1 + \xi_2(2x_S + x_M + x_F + \frac{3}{5}x_B) + \nu', \quad \textbf{(8)}$$

$$\hat{\gamma} = \xi_1 + \xi_2(2x_S + x_M + x_F + \frac{3}{5}x_B) + \nu'', \quad \textbf{(9)}$$

where

- $\hat{\alpha}$, $\hat{\beta}$ and $\hat{\gamma}$ are respectively the estimation α, β, γ
- x_S (resp. x_M, x_F, x_B) are the proportion of skin (resp., muscles, fat and bones) to the body mass.
- ξ_1 and ξ_2 are the parameters of the surrogate models (7), (8) and (9)
- ν, ν' and ν'' are the errors generated by the models (7), (8) and (9)respectively

The tissues weightings in the formula (i.e. $(2x_S + x_M + x_F + \frac{3}{5}x_B)$) are established empirically from observations made on models (7), (8) and (9).

The unknown parameters ξ_1 and ξ_2 are estimated by the least square method. For this purpose, the parameters $(\alpha_i)_{i=1,...,12}$, $(\beta_i)_{i=1,...,12}$ and $(\gamma_i)_{i=1,...,12}$ of the phantom are calculated using (4), (5) and (6) and injected in (7), (8) and (9). The results of the estimations are in table 4.

Table 5. Estimation of the parameters of surrogate models (7), (8) and (9), and the coefficient of determination.

	ξ_1	ξ_2	Max. relative error (%)	R^2
α Surrogate Model (8)	1.15	-1.05	11.46%	0.89
β Surrogate Model (9)	0.55	-0.46	8.95%	0.87
γ Surrogate Model(10)	0.14	-0.13	13.02%	0.88

The maximal relative error for these models varies between 9% and 13%. To study the stability of coefficients ξ_1 and ξ_2, we propose to estimate these parameters with only 9 phantoms instead of 12. All combinations of the 9 phantoms out of 12 are tested to validate the robustness of the estimation. We notice that the parameters are relatively stable (only 5% of variability) for the surrogate models (7) and (9) while, the surrogate model (8) is about 11%. This could stem from the fact that certain phantoms (experiences) can be very influential. To measure this influence of experiences, the distance of Cook [Saporta 1990] is computed. A Cook distance close to 1 means that the phantom is very influential. The following table shows the distance of Cook computed for each phantom using the three surrogate models (7), (8) and (9).

Table 6. The distance of Cook measured for each phantom and each surrogate model

	S. model (8)	S. model (9)	S. model (10)
Norman	0.68	0.06	0.163
Japanese male	0.006	0.0072	0.009
Korean	0.09	**0.94**	0.012
Zubal	0.0001	0.003	0.0001
VH	0.078	0.02	0.12
Japanese Female	0.15	0.12	0.13
Ella	0.093	0.005	0.135
Duke	0.045	0.014	0.035
Billie	0.046	0.56	0.007
Thelonious	0.002	0.0003	0.002
Naomi	0.07	0.003	0.07
HDRK	0.003	0	0.005

The results of the table 6 show that the distance of Cook obtained for the Korean for the surrogate model (8) is close to 1. This means that the Korean is very influential, for this surrogate model (8).

Hence, if the Korean model is forced to be a common sample (8 random + Korean) for the stability test (9 among 12), the variability is reduced to 5%.

In addition, when extrapolation from each set of 9 models to 12 models, the maximal relative error is 13.14%, 8.1% and 14.6% for the surrogate models (7), (8) and (9) respectively. This means that the built surrogate models are robust.

4. Conclusion

To characterize the statistical distribution of the WBSAR for given population, surrogate models are built in terms of the morphology. These surrogate models are based on the proportionality between the absorbed power and the surface of the human body.
This study is based on anatomical phantoms standing and exposed to a plane wave polarized vertically and arriving in front of them at the frequency of 2100 MHz.
This study shows that both internal and external morphology are equally important in the construction of a surrogate model of the WBSAR. Indeed, the different models established with only external morphological factors (such as the body surface area, the body mass index and the weight) generate an important error on the estimation of the WBSAR (about 30% in term of relative error).
Nevertheless, these surrogate models give a good estimation of the WBSAR when the families of phantoms (original phantom + morphed phantoms) are considered. The observations made on these families show that the proportions of the different tissues (such as the proportion of muscle and bones…) are quasi equal. This analysis stresses the importance of the internal morphological factors.
To reduce the error estimation of the surrogate models the internal factors were introduced. Then the error is reduced to 10%. Furthermore, the study of the stability of these surrogate models using all the combinations of nine phantoms among twelve show that the given models are robust.
Since the internal morphological factors are influent on the WBSAR, The statistical distribution of the WBSAR is very difficult to obtain for a given population. In fact, the statistical data concerning the internal morphology are impossible to obtain and the type of dependency between external and internal morphology is ignored.
The objective is to consider the parameters of the internal morphology as a random variable in which internal morphology of the phantoms are considered as a random sampling. Nevertheless these phantoms are not sufficient to correctly describe the distribution of this random variable for a given population.
The analysis has been carried out at the frequency of 2.1 GHz. Nevertheless, the same methodology can be applied at high frequency.
Our perspectives are firstly to validate the surrogate models established in this study using new phantoms. And finally to characterize the statistical distribution of the term of internal morphology. For this purpose, the information provided by our phantoms and the expert knowledge (on phenomenon of wave absorption by the human body tissues) will be integrated. The obtain result will allow to extrapolate the WBSAR for populations characterized by its external morphology.

5. References

Ackerman MJ. 1995 Accessing the Visible Human Project *D Lib Mag* available from http://www.nlm.nih.gov/research/visible/visible_human.html

Berenger JP. 1994. A perfectly matched layer for the absorption of electromagnetic waves. *J Comput Phys* **4**:185–200.

Conil. E, Hadjem. A, Lacroux. F, Wong. MF and Wiart J 2008 Variability analysis of SAR from 20MHz to 2.4GHz for different adult and child models using FDTD Phys. *Med. Biol*.**53** 1511-1525.

Conil E, Hadjem A, Gati A, Wong M-F, and Joe Wiart 2009, " Influence of the plane wave's incidence on the whole body exposure at 2100MHz", submitted to *IEEE EMC*

Christ A, Kainz W; Hahn E, Honegger K, Shen J, Rascher W, Janka R, Bautz W, Kiefer B, Schmitt P, Hollenbach H, Chen J, Kam A, Neufeld E, Oberle M and Kuster N. "The Virtual Family Project - Development of Anatomical Whole-Body Models of Two Adults and Two Children". *Proceedings of the 23rd Annual Review of Progress in Applied Computational Electromagnetics* (ACES) 2007, 2007.

Dimbylow PJ. 1997. FDTD calculations of the whole-body averaged SAR in an anatomically realistic voxel model of the human body from 1 MHz to 1 GHz. *Phys Med Biol* **42**: 479-90

Dimbylow P. 2005a. Resonance behaviour of whole-body averaged specific energy absorption rate (SAR) in the female voxel model, NAOMI. Phys. Med. Bio. 50: 4053-4063.

DuBois D & DuBois EF 1916 A formula to estimate the approximate surface area if height and weight be known *Arch Int Med* 17:863-71

Gandhi, O.P."State of the knowledge for electromagnetic absorbed dose in man and animals"; Proceedings of the IEEE Volume 68, Issue 1, Jan. 1980 Page(s):24 – 32

Hadjem A, Lautru D, Dale C, Wong M F, Hanna V F and Wiart J 2004 Comparison of specific absorption rate (SAR) induced in child-sized and adult heads using a dual band mobile phone *IEEE-MTT-S Int. Microwave Symp. Dig* pp 1453-6

Hirata A, Fujiwara O, Nagaoka T, Watanabe S, 2008 "Estimation of Whole-Body Average SAR in Human Models Due to Plane-wave Exposure et Resonance Frequency".

Hirata A, Nagaya Y, Fujiwara O, 2007 " Correlation between Absorption Cross Section and Body Surface Area of Human for Far-Field Exposureat GHz Bands".

ICNIRP 1998 Guidelines for Limiting Exposure to Time Varying Electric Magnetic and Electromagnetic Field (up to 300 GHz). *Radiation Protection Health Physics*, Volume **74**, Number 4:494-522

Kim, J. I.; Choi, H.; Lee, B. I.; Lim, Y. K.; Kim, C. S.; Lee, J. K.; Lee, C. 2006 Physical phantom of typical Korean male for radiation protection purpose. *Radiation Protection Dosimetry*, Volume **118**, Number 1, pp. 131-136

Kim C H, Choi S H, Jeong J H, Lee Cand Chung M S. 2008. HDRK-man a Whole body voxel model based on high resolution color slice images of a Korean adult male cadaver.*Phys.Med.Bio*, VOl **53**, 4093-4106.

Kühn S, Jennings W, Christ A and Kuster N. 2009. Assassement of induced radio-frequency electromagnetic fields in various human body models. Phys. Med. Biol. vol **54**. 875-890.

Lee A, Choi W Y, Chung M S, Choi H D, And Choi J I Developement of Korean male body model for computational dosimetry *ETRI J.* **28** 107-10

Lim TO., Ding LM., Zaki M., Suleiman AB., Fatimah S., Tahir A., Mainmunah AH., 2000 "Distribution of body weight, height and body mass index in national sample of Malayesian Adults". *Med J Malaysia* , vol **55:** 108-128

Livingston EH., Lee S., "Body Surface Area prediction in normal-weight and obese patients", 2001,*Am J Physiol Endocrinol Metab*, Vol **281**, Issue 3, E586-E591.

Nagaoka T, Watanabe S, Sakurai K, Kunieda E, Taki M, Yamanaka Y. Development of realistic high-resolution whole-body voxel models of Japanese adult males and females of average height and weight, and application of models to radio-frequency electromagnetic-field dosimetry. *Phys Med Biol* **49** (2004): 1-15

Pineau J C and Kapitanik B, " Les français ages de 20 ans : relation entre le deficit ou l'excedent pondéral et le body mass index (BMI)", 2004. *Antropo*, vol 8, 93-100. www.didac.ehu.es/antropo

Pressinitto E, Pisent C, Sergi G, Grigoletto F, Enzi G, 2002 Anthropometric measurements in elderly: age and gender difference *British Journal of Nutrition*, **87**, 177-186.

Saporta G Probabilités, analyse de données et statistiques, *Gulf Publishing Company*, January 1990.

Taflove A & Hagness S, Computational Electrodynamics. *Artech House* Ed. 2000 ISBN isbn 1-58053-076-1.

Visible Human Project National Library of Medicine 8600 Rockville Pike Bethesda, MD 2089 4 www.nlm.nih.gov/ research/visible

Wang J, Fujiwara O, Kodera S and Watanabe S 2006b FDTD calculation of whole-body average SAR in adult and child models for frequencies from 30vMHz to3 GHz *phys. Med. Biol* **51** 4119-27

Yee K S, 1966 Numerical solution of initial boundary value problems involving Maxwell's equations in isotropic media. *IEEE Trans. Antennas Propagat.*, vol. **14**, no. 3, pp. 302-307.

Zubal IG, Harrell CR, Smith EO, Rattner Z, Gindi G, Hoffer BP. 1994. Computerized 3-dimensional segmented human anatomy. *Med Phys* **21**: 299-302.